

Persistent currents in mesoscopic rings: A numerical and renormalization group study

V. Meden

Institut für Theoretische Physik, Universität Göttingen, Bunsenstr. 9, D-37073 Göttingen, Germany

U. Schollwöck

Max-Planck-Institut für Festkörperforschung, Heisenbergstr. 1, D-70569 Stuttgart, Germany

(September 25, 2002)

The persistent current in a lattice model of a one-dimensional interacting electron system is systematically studied using a complex version of the density matrix renormalization group algorithm and the functional renormalization group method. We mainly focus on the situation where a single impurity is included in the ring penetrated by a magnetic flux. Due to the interplay of the electron-electron interaction and the impurity the persistent current in a system of N lattice sites vanishes faster than $1/N$. Only for very large systems and large impurities our results are consistent with the bosonization prediction obtained for an effective field theory. The results from the density matrix renormalization group and the functional renormalization group agree well for interactions as large as the band width, even though as an approximation in the latter method the flow of the two-particle vertex is neglected. This confirms that the functional renormalization group method is a very powerful tool to investigate correlated electron systems. The method will become very useful for the theoretical description of the electronic properties of small conducting ring molecules.

71.10.Pm, 73.23.Ra, 73.63.-b

I. INTRODUCTION

The experimental observation of persistent currents in mesoscopic metallic and semiconducting rings pierced by a magnetic flux¹⁻⁶ has led to many theoretical investigations focusing on the interplay of electron-electron interaction and disorder in such systems.⁷ This interplay is considered to be one of the possible reasons for the large current observed in the experiments.⁷ Despite these studies a quantitative theoretical understanding of the observed amplitude of the currents for the three-dimensional rings is still missing. To gain theoretical insight the simplified situation of one-dimensional rings with interaction and disorder was studied using exact diagonalization for systems of very few lattice sites (up to 16)⁸⁻¹⁰ and the self-consistent Hartree-Fock approximation.^{10,11} Here we consider the further simplified problem of the persistent current in a one-dimensional ring of interacting electrons in the presence of a single impurity and penetrated by a magnetic flux. Within an effective continuum field theory it has theoretically been investigated using bosonization¹² and conformal field theory.^{13,14} At first glance this problem seems to be of purely academic interest, but the fast progress in the design and manipulation of conducting ring molecules gives a perspective that such systems might be accessible to experiments in the very near future.

For a continuum model of non-interacting one-dimensional electrons the leading behavior of the persistent current $I(\phi)$ in the system size L can be calculated in the presence of an arbitrary potential scatterer.¹² It is a periodic function of the flux, vanishes as $1/L$, and its shape and size are determined by the absolute value

of the transmission amplitude $|T(k_F)|$ of the potential at the Fermi wave vector k_F . For a vanishing impurity, i.e. $|T(k_F)| \rightarrow 1$, $I(\phi)$ has a saw tooth like shape, which gets rounded off if $|T(k_F)|$ is decreased. In the limit of small $|T(k_F)|$, $I(\phi)$ is proportional to $|T(k_F)| \sin \phi$. For the tight-binding lattice model supplemented by a single weak hopping matrix element the persistent current at half-filling can also be calculated analytically¹³ and the same characteristics can be found (see Sect. II).

Compared to the Fermi liquid behavior of higher dimensional systems a large class of models of homogeneous one-dimensional interacting electrons has a significantly different low-energy physics. These models belong to the Luttinger liquid universality class.¹⁵ The low-energy excitations of Luttinger liquids are not given by fermionic quasi-particles, but are of collective, bosonic nature. This leads e.g. to a typical power-law decay of correlation functions. The low-energy physics of Luttinger liquids is characterized by a set of interaction and filling factor dependent parameters.¹⁵ For the case of spinless fermions on which we focus any pair of the four parameters v_J (velocity of current excitations), v_N (velocity relevant if particles are added), v_c (velocity of charge excitations at constant number of particles), and the Luttinger liquid parameter K can be used. Within bosonization and for the impurity free case the persistent current in a Luttinger liquid is periodic in ϕ and of saw tooth like shape with slope $v_J/(\pi L)$.¹⁵⁻¹⁷ In Sect. III we will compare our numerical results to this prediction.

The low-energy physics of Luttinger liquids is strongly affected by the presence of a single impurity.¹⁸⁻²³ The problem is usually mapped onto an effective continuum field theory using bosonization, where terms which are

expected to be irrelevant in the low-energy limit are neglected.^{18–22} Within this field theory the leading L dependence of the persistent current was obtained by an additional self-consistent approximation using the analogy to the problem of quantum coherence in a dissipative environment.¹² This approach gives a current which for large L vanishes as $L^{-\alpha_B-1}$, with $\alpha_B = 1/K - 1$, and independent of the bare impurity strength is of purely sinusoidal shape.¹² For repulsive interaction one has $K < 1$ and thus $\alpha_B > 0$. α_B is also the exponent of the power-law suppression (as a function of energy) of the local spectral weight close to an open boundary and the chemical potential.^{21,24} This explains the index B which stands for boundary. Many of the bosonization results for observables which are dominated by the interplay of a single impurity and the electron-electron interaction can be understood in terms of a single particle picture, which for Luttinger liquids has of course to be used with caution: For large L the effective transmission amplitude near the Fermi points is suppressed with respect to the non-interacting transmission by a factor of $L^{-\alpha_B}$. Combining this with the behavior of the persistent current in the non-interacting case the above result, obtained without the use of the single particle language, can be derived.

For several reasons it is desirable to directly show the above behavior of the persistent current in microscopic lattice models avoiding bosonization. Mapping such models on the field theory involves approximations. Their validity can be questioned and they lead to a loss of information; the scales of the microscopic model and corrections to the expected power-law scaling hidden in the irrelevant terms are lost. Furthermore even within the field theory an additional approximation is necessary to determine the leading (in the system size) behavior of the persistent current. A knowledge of the detailed shape of $I(\phi)$ beyond the leading behavior and for microscopic models is of special importance if one wants to compare theoretical results to experiments. Several attempts have been made in this direction using the model of spinless fermions with nearest neighbor hopping and interaction. Here we also focus on this model. The persistent current can be calculated by taking the derivative of the groundstate energy $E_0(\phi)$ with respect to the flux ϕ penetrating the ring. Instead of calculating the full functional form of $I(\phi)$ the so called phase sensitivity ΔE_0 , which is the difference of the groundstate energy at flux 0 and π has numerically been determined using the density matrix renormalization group (DMRG) method.^{25,26} The phase sensitivity can be considered a crude measure for the persistent current, but of course does not contain information on the detailed shape of the current as a function of ϕ . Very recently ΔE_0 has again been studied numerically using DMRG and the quantum Monte Carlo method.²⁷ ΔE_0 instead of $I(\phi)$ (which implies calculating $E_0(\phi)$ for several ϕ and numerically taking the derivative) is calculated because this way the hamiltonian matrix remains real and the numerical effort is reduced considerably.²⁸ Here we use complex DMRG to

calculate $I(\phi)$ with very high precision and for systems of up to $N = 128$ lattice sites.²⁹ Additionally the functional renormalization group (RG) method introduced recently into the theory of strongly correlated electrons is used.^{30,31} It has been applied to two-dimensional correlated electron systems³² and one-dimensional Luttinger liquids.^{33–35} We have used this method before to study a local observable^{33,34} - the local spectral weight close an impurity - which is also dominated by the interplay of electron-electron interaction and impurity. In contrast the persistent current is a property of the entire system. Within the RG approach the flow equations are closed by neglecting the flow of the two-particle vertex. Nonetheless DMRG and RG agree quantitatively for interactions of the order of the band width. This confirms that the functional RG is a very powerful tool to investigate strongly correlated electrons. For the single impurity case we indeed find that the persistent current vanishes faster than N^{-1} . To analyze $NI(\phi)$ in more detail we expand the current in a Fourier series, demonstrate that for large impurities and very large system sizes the behavior of the first Fourier coefficient is consistent with a power-law decay with exponent $-\alpha_B$, and that the higher order coefficients decay even faster. Thus in the $N \rightarrow \infty$ limit $I(\phi)$ is proportional to $\sin\phi$ with an amplitude which vanishes as $N^{-\alpha_B-1}$. However, this universal bosonization prediction only holds for very long chains respectively very large impurities. For smaller systems and impurities the asymptotic limit is not reached and the current displays a more complex behavior. It can quantitatively be described using the functional RG method. This makes the method an ideal tool to investigate the electronic properties of small, one-dimensional molecular rings which might be experimentally accessible very soon.

II. THE MODEL

The Hamiltonian for the impurity free ring penetrated by a magnetic flux ϕ (measured in units of the flux quantum $\phi_0 = hc/e$) with nearest neighbor interaction U is given by

$$H = - \sum_{j=1}^N \left(c_j^\dagger c_{j+1} e^{i\phi/N} + c_{j+1}^\dagger c_j e^{-i\phi/N} \right) + U \sum_{j=1}^N n_j n_{j+1}, \quad (1)$$

in standard second-quantized notation. The hopping matrix element and the lattice constant are set to one and periodic boundary conditions are used. For $U = 0$ the groundstate energy of the model can easily be calculated. At temperature $T = 0$ and for fixed N the persistent current follows from $E_0(\phi)$ by taking the derivative with respect to ϕ

$$I(\phi) = -\frac{dE_0(\phi)}{d\phi} \quad (2)$$

as can be shown using the Hellman-Feynman theorem. To leading order in $1/N$ this gives

$$I(\phi) = -\frac{v_F}{\pi N} \times \begin{cases} \phi & \text{for } N_F \text{ odd and } -\pi \leq \phi < \pi \\ \phi - \pi & \text{for } N_F \text{ even and } 0 \leq \phi < 2\pi, \end{cases}$$

where v_F denotes the Fermi velocity and N_F is the number of particles.³⁶ Both functions have to be continued periodically. Eq. (2) also holds for non-vanishing interaction and if impurity terms are added. The above even-odd effect can also be observed if interaction and impurities are included. We from now on only consider even N_F .

At $\phi = 0$ the Luttinger liquid parameter K and the velocity of current excitations v_J of the model Eq. (1) can be determined using the Bethe ansatz.³⁷ For half-filling the resulting integral equations have been solved analytically with the results

$$K = \left[\frac{2}{\pi} \arccos(-U/2) \right]^{-1} \quad (3)$$

and ($v_J = v_c K$)

$$v_J = \pi \frac{\sqrt{1 - (U/2)^2}}{\pi - \arccos(-U/2)} \left[\frac{2}{\pi} \arccos(-U/2) \right]^{-1}. \quad (4)$$

For this filling the model is a Luttinger liquid for $-2 < U \leq 2$. At $|U| = 2$ the model shows phase transitions to a charge density wave groundstate ($U = 2$) and a phase separated state ($U = -2$). To leading order in $1/N$ the bosonization prediction for the persistent current in a homogeneous Luttinger liquid is a saw tooth like curve with slope $-v_J/(\pi N)$, i.e. compared to the non-interacting case v_F is replaced by the velocity determining the current excitations. To compare our data with this result also away from half-filling we numerically solved the Bethe ansatz integral equations following Refs. 37 and 38 and determined v_J (see Sect. III). In our study we will always stay in the Luttinger liquid phase.

To H we add a hopping impurity

$$H_h = (1 - \rho) \left(c_N^\dagger c_1 e^{i\phi/N} + c_1^\dagger c_N e^{-i\phi/N} \right). \quad (5)$$

with ρ between 0 (no hopping between sites N and 1) and 1 (no impurity). In the non-interacting limit, at half-filling, and at wavevector k_F the transmission coefficient of the hopping impurity (for $N \rightarrow \infty$) is given by³⁹

$$|T(k_F)|^2 = \frac{4\rho^2}{(1 + \rho^2)^2}, \quad (6)$$

which provides us with a measure for the strength of the impurity. For $U = 0$, $N_F = N/2$, and to leading order in $1/N$ the persistent current of the hamiltonian $H + H_h$ has been calculated using conformal field theory.¹³ To

obtain $I(\phi)$ it is not necessary to use this field theoretical approach since Eq. (7) of Ref. 13 which determines the allowed wave vectors can be solved directly. Written in terms of $|T(k_F)|$ the current is given by

$$I(\phi) = \frac{v_F}{\pi N} \frac{\arccos(|T(k_F)| \cos[\phi - \pi])}{\sqrt{1 - |T(k_F)|^2 \cos^2 \phi}} |T(k_F)| \sin \phi, \quad (7)$$

which is exactly the expression obtained in Ref. 12 for the continuum model. Later we will be interested in the small $|T(k_F)|$ limit. Therefore we expand Eq. (7) up to third order in $|T(k_F)|$

$$\begin{aligned} NI(\phi) &= \frac{v_F}{2} |T(k_F)| (1 + |T(k_F)|^2/8) \sin(\phi) \\ &+ \frac{v_F}{2\pi} |T(k_F)|^2 \sin(2\phi) \\ &+ \frac{v_F}{16} |T(k_F)|^3 \sin(3\phi) + \mathcal{O}(|T(k_F)|^4), \quad (8) \end{aligned}$$

which at the same time gives an expansion in a Fourier series. The expansion explicitly shows that in the limit $|T(k_F)| \rightarrow 0$ of a strong impurity the current becomes more and more of sinusoidal shape.

A simple approximation which allows to study the effect of the interaction and impurity on the persistent current simultaneously is the Hartree-Fock approximation. For the bulk properties of homogeneous one-dimensional correlated electron systems this approximation does not capture any of the Luttinger liquid features and is thus of very limited usefulness. Furthermore, when applying the self-consistent Hartree-Fock approximation to a model with a single impurity, the self-consistent iterative solution of the Hartree-Fock equations will drive the system into a charge density wave groundstate with a finite single-particle gap which is qualitatively incorrect since a single impurity cannot change bulk properties of the system. Nevertheless self-consistent Hartree-Fock has been used to determine the persistent current in one-dimensional, interacting, and disordered rings^{10,11} and also for the single impurity case.¹¹ In contrast if one is interested in the local properties close to a boundary or impurity non-self-consistent Hartree-Fock provides useful informations.^{24,33,34} In Sect. V we also present results for the persistent current calculated within the non-self-consistent Hartree-Fock approximation. They were obtained by numerically determining the groundstate of $H + H_h$ for $U = 0$ and fixed ϕ and N . From this the expectation values $\langle n_j \rangle_0$ and $\langle c_{j+1}^\dagger c_j \rangle_0$, which determine the mean-field hamiltonian H_{MF} , can be calculated. H_{MF} can then be diagonalized numerically. There are two possibilities to determine the groundstate energy within this approximation. One can either take the Slater determinant expectation value of $H + H_h$ using the groundstate of H_{MF} or determine the energy via the one-particle propagator⁴⁰ by the formula

$$\begin{aligned}
\langle H + H_h \rangle_{\text{MF}} = & \frac{1}{2} \left[- \lim_{\tau' \rightarrow \tau} \sum_{j=1}^N \left\langle c_j^\dagger(\tau') \frac{d}{d\tau} c_j(\tau) \right\rangle_{\text{MF}} \right. \\
& - \sum_{j=1}^N \left(e^{i\phi/N} \left\langle c_j^\dagger c_{j+1} \right\rangle_{\text{MF}} + \text{c.c.} \right) \\
& \left. + (1 - \rho) \left(e^{i\phi/N} \left\langle c_N^\dagger c_1 \right\rangle_{\text{MF}} + \text{c.c.} \right) \right] \quad (9)
\end{aligned}$$

where the expectation values are taken using the groundstate of H_{MF} . $c_j^{(\dagger)}(\tau)$ denotes the annihilation (creation) operator in the imaginary time Heisenberg representation. Transforming the first term into the Matsubara frequency representation it can be written as $\sum_{l=1}^{N_F} \varepsilon_l^{\text{MF}}$, with the eigenenergies $\varepsilon_l^{\text{MF}}$ of H_{MF} . Only if the self-consistent Hartree-Fock approximation is used, which for the reason given above we do not consider in the present context, both possibilities give the same result. Formally both approximations to the energy are correct to leading order in U , but it turned out that the latter method gives better results compared to the high-precision DMRG data. For the results presented in Sec. V we thus used Eq. (9). There it will be shown that the currents calculated using the Hartree-Fock approximation are qualitatively wrong, since in this method correlation effects are neglected which in the present context are of great importance.

III. COMPLEX DMRG

Using the DMRG algorithm the groundstate energy of an interacting one-dimensional many fermion system can be calculated to high precision.⁴¹ To determine the persistent current using Eq. (2) for the hamiltonian $H + H_h$ [Eqs. (1) and (5)] the DMRG procedure has to be generalized to complex hamiltonian matrices. Calculation time scales up by about a factor of 4, memory usage by a factor of 2. This limits the performance of the method, which is however numerically very stable as hermiticity is conserved. We have kept up to 400 states, ensuring that energies and derived currents are essentially exact.

As a test of our program we first studied the impurity free case given by the hamiltonian Eq. (1). We calculated the groundstate energy as a function of ϕ for $0 \leq \phi \leq \pi$. Results for quarter-filling $n = 1/4$, $N = 64$ and $U = 0.5, 1, 1.5$ are shown in Fig. 1. Bosonization predicts that to leading order in $1/N$ the current is given by

$$I(\phi) = -\frac{v_J}{\pi N}(\phi - \pi) \quad (10)$$

and thus the groundstate energy by

$$E_0(\phi) = \text{const.} + \frac{v_J}{2\pi N}(\phi - \pi)^2. \quad (11)$$

As shown in Fig. 1 the DMRG data nicely lie on curves of this form with the constant and the current velocity

as fit parameters. In Fig. 2 the $v_J^{\text{DMRG}}(n, U)$ extracted from such fits are compared to the exact $v_J(n, U)$ obtained from the Bethe ansatz. Data for $n = 1/4$ (with $N = 64$) and $n = 1/2$ (with $N = 60$) and different U are shown. For both fillings the Bethe ansatz and DMRG results are indistinguishable on the scale of the plot. The relative error of the DMRG data is of the order of 10^{-4} . This confirms the bosonization prediction, shows that the complex DMRG can be applied successfully, and that the current velocity can to very high precision be extracted from finite size data as small as 60 lattice sites without using finite size scaling. In Ref. 25 data for the phase sensitivity of the translational invariant model at half-filling were obtained using DMRG. Our results for $v_J^{\text{DMRG}}(n = 1/2, U)$ are consistent with the ones presented there. As seen in Fig. 2 the dependence of v_J on U gets weaker if the filling is getting smaller. This happens because for smaller fillings the lattice model is closer to the electron gas model with quadratic dispersion. The latter model is Galilean-invariant which leads to $v_J = v_F$ independent of the interaction.

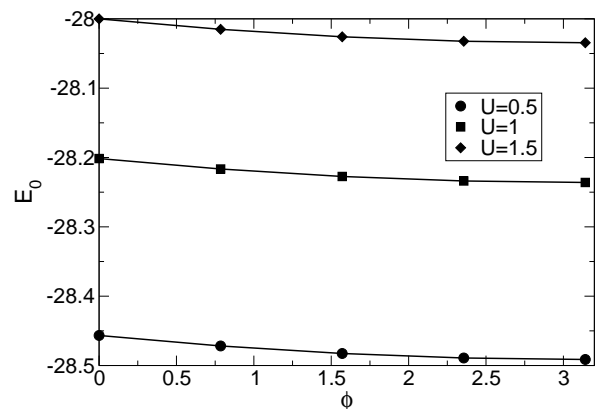


FIG. 1. Groundstate energy as a function of the flux ϕ for quarter-filling, $N = 64$, and different U . The symbols are DMRG data and the lines are quadratic fits (see the text).

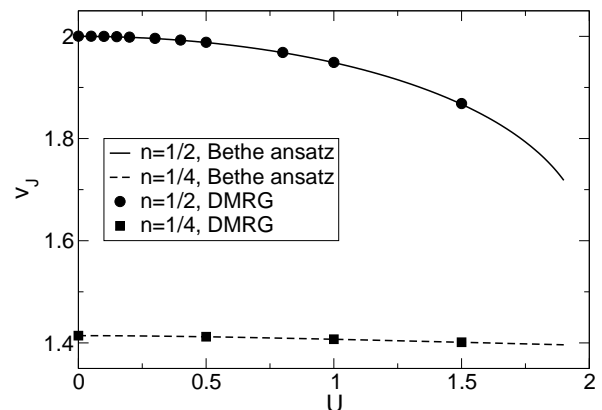


FIG. 2. Current velocity $v_J(n, U)$ as obtained from the Bethe ansatz and from the DMRG.

IV. RG METHOD

Besides DMRG we will also use the functional RG method in the version using one-particle irreducible vertex functions.^{30,31} In collaboration with W. Metzner and K. Schönhammer we have successfully applied this method in the past to determine the local spectral weight of a Luttinger liquid close to an open boundary and an impurity.^{33,34} In the method one introduces a cut-off parameter Λ in the non-interacting propagator G^0 cutting out degrees of freedom on energy scales less than Λ and derives an exact hierarchy of coupled differential flow equations for the one-particle irreducible vertex functions by differentiating with respect to Λ , where Λ flows from ∞ to 0.

For $\phi = 0$ the flow equation for the selfenergy⁴² of the hamiltonian $H + H_h$ has been given in Ref. 34. As in this reference we here also neglect the flow of the two-particle vertex which closes the set of differential equations; this leads to a energy independent selfenergy. Within the approximation the results obtained are at least correct to leading order in U , but our work presented in Refs. 33 and 34 shows that the Luttinger liquid scaling of the impurity (i.e. the transmission) is included, which makes the RG a promising method also in the present context.

If a frequency cutoff

$$G^{0,\Lambda}(i\omega) = \Theta(|\omega| - \Lambda)G^0(i\omega) \quad (12)$$

is used, the set of flow equations for the selfenergy³⁴ in the Wannier basis is given by

$$\frac{d}{d\Lambda}\Sigma_{j,j}^\Lambda = -\frac{U}{2\pi} \sum_{s=\pm 1} \sum_{\omega=\pm\Lambda} G_{j+s,j+s}^\Lambda(i\omega) \quad (13)$$

$$\frac{d}{d\Lambda}\Sigma_{j,j\pm 1}^\Lambda = \frac{U}{2\pi} \sum_{\omega=\pm\Lambda} G_{j,j\pm 1}^\Lambda(i\omega), \quad (14)$$

with

$$G^\Lambda(i\omega) = \left\{ [G^0(i\omega)]^{-1} - \Sigma^\Lambda \right\}^{-1}. \quad (15)$$

In Eqs. (13) and (14) the flow from $\Lambda = \infty$ down to a scale Λ_0 much larger than the band width has already been included. The flow is continued from Λ_0 downwards with the initial conditions

$$\begin{aligned} \Sigma_{j,j}^{\Lambda_0} &= U, \quad 1 \leq j \leq N \\ \Sigma_{j,j\pm 1}^{\Lambda_0} &= 0, \quad 1 < j < N \\ \Sigma_{1,N}^{\Lambda_0} &= (1 - \rho) e^{-i\phi/N} = \left(\Sigma_{N,1}^{\Lambda_0} \right)^*. \end{aligned} \quad (16)$$

In contrast to the situation studied in Refs. 33 and 34 the matrix elements $\Sigma_{j,j\pm 1}^\Lambda$ are complex numbers which increases the size of the set of differential equations. Furthermore we here have to use periodic boundary conditions so that $G^\Lambda(i\omega)$ is not tridiagonal.

The set of Eqs. (13) and (14) is complemented by a differential equation for the “zero-particle” vertex γ_0 (with the Boltzmann constant k_B set to one)

$$\lim_{T \rightarrow 0} T \frac{d}{d\Lambda} \gamma_0^\Lambda = \frac{1}{2\pi} \text{Tr} \left[\sum_{\omega=\pm\Lambda} \ln \{ 1 - G^0(i\omega) \Sigma^\Lambda(i\omega) \} \right], \quad (17)$$

where Tr denotes the trace over the indices of the Wannier basis states. The initial condition is $\gamma_0^{\Lambda=\infty} = \gamma_0^{\Lambda_0} = 0$. Eq. (17) also holds if the flow of the two-particle vertex and all higher vertices are taken into account. The flow of γ_0^Λ only couples to the selfenergy. It does not feed back to any higher order vertex function. $\gamma_0 = \gamma_0^{\Lambda=0}$ is related to the grand canonical potential Ω by

$$\Omega = T\gamma_0 + \Omega_0, \quad (18)$$

where Ω_0 is the grand canonical potential at $U = 0$. From Ω the ground state energy can be obtained in the $T \rightarrow 0$ limit

$$\begin{aligned} E_0(\phi) - \mu \langle \hat{N} \rangle &= \Omega(T = 0) \\ &= \lim_{T \rightarrow 0} T\gamma_0 + E_0^0(\phi) - \mu_0 \langle \hat{N} \rangle_0. \end{aligned} \quad (19)$$

\hat{N} is the particle number operator and μ the chemical potential. The quantities with an additional index 0 are taken at $U = 0$. Eqs. (18) and (19) make explicit that the functional RG is a grand canonical method. In general to obtain the persistent current within a grand canonical ensemble corrections to Eq. (2) have to be taken into account since the chemical potential can dependent on the flux.^{43,44} For half-filling and a single hopping impurity μ is always fixed at U (and μ_0 at 0) and thus we do not have to worry about this issue if we use the RG only for $n = 1/2$.

The set of differential equations (13), (14), and (17) can be solved numerically for a fixed N and ϕ . Additionally $E_0^0(\phi)$ can be calculated by numerically diagonalizing the one-particle problem at $U = 0$. Thus $E_0(\phi)$ can be determined. There are two factors which limit the system sizes that can be treated numerically. On the right hand side of the flow equations a $N \times N$ matrix has either to be inverted or to be diagonalized. This limits N to a few thousand lattice sites. The more restrictive limit comes from the fact that within the ground state energy which is proportional to N one is interested in the ϕ dependence which vanishes faster than $1/N$ (see above and the next section). Thus the differential equations have to be solved with extremely high precision. For this reason we here only consider systems of up to $N = 256$ lattice sites. It is worth noting that for a given N the RG method with the approximation as we use it is still much faster than the “numerically exact” DMRG.

An alternative way to determine $E_0(\phi)$ would be to use Eq. (9) with the mean-field expectation values replaced

by the ones determined at $\Lambda = 0$. Formally the use of the flow equation for γ_0 and this method are correct to leading order in U but it turned out that calculating $E_0(\phi)$ from $\gamma_0^{\Lambda=0}$ gives much better results compared to the accurate DMRG data. For the results presented in the next section we thus used Eqs. (17) and (19). There we will demonstrate that the RG data agree quantitatively with the DMRG data for U as large as the band width.

V. RESULTS

In this section we present our results for the persistent current including interaction and a hopping impurity obtained from DMRG and RG. To demonstrate that the Hartree-Fock approximation should not be used in the present context we also show results obtained using this approximation. We here exclusively consider $n = 1/2$. In the DMRG and RG we have calculated $E_0(\phi)$ for $0 < \phi \leq \pi$ at 20 different ϕ_l and used the symmetry of the data to extend them to the periodicity interval $-\pi < \phi \leq \pi$. From these data we have determined $I(\phi)$ using numerical differentiation. To make sure that the error obtained from this is small we have not only used simple centered differences but also applied an approximation scheme using Chebychev polynomials.⁴⁵ This explains why the ϕ_l are not equidistant (see Figs. 3 to 5). Up to very small differences both methods give the same current.

In Fig. 3 $NI(\phi)$ is presented for $U = 1$ and $\rho = 0.5$, which for $U = 0$ corresponds to a transmission $|T(k_F)|^2 = 0.64$, and different N . Additionally the leading $1/N$ behavior at $U = 0$ [Eq. (7)] is shown as a dashed line. As is obvious the interplay of interaction and impurity leads to a current which vanishes faster than $1/N$. The DMRG and RG data agree quantitatively, which shows that the functional RG provides a very good approximation (for a fairly large U) even if the flow of the vertex is neglected. The Hartree-Fock approximation gives qualitatively wrong results. This shows that correlation effects not taken into account by Hartree-Fock are very important. We thus do not consider this approximation any further. For $U = 1.733333$, i.e. close to the phase transition into a charge density wave groundstate, the DMRG and RG data are shown in Fig. 4 for the same ρ . For this larger U the suppression is even stronger but the RG data still show an excellent agreement with the high precision DMRG results.

As discussed in the introduction in the large N limit bosonization predicts that $I(\phi)$ is suppressed by a factor $N^{-\alpha_B-1}$ instead of N^{-1} and proportional to $\sin \phi$. With increasing U , α_B gets larger and one thus expects this asymptotic regime to be reached faster. Even though we observe a suppression which is stronger than N^{-1} from Figs. 3 and 4 it is not clear whether a power-law behavior is realized. Furthermore the data even for $U = 1.733333$ are still far from being proportional to $\sin \phi$. For a

stronger impurity, i.e. smaller ρ the asymptotic regime should also be reached faster since already the non-interacting current is closer to a sinusoidal shape. This is demonstrated in Fig. 5 for $U = 1$ and $\rho = 0.25$. The $U = 0$ transmission for $\rho = 0.25$ is $|T(k_F)|^2 = 0.22$, i.e. this case corresponds to an already fairly strong (bare) impurity.

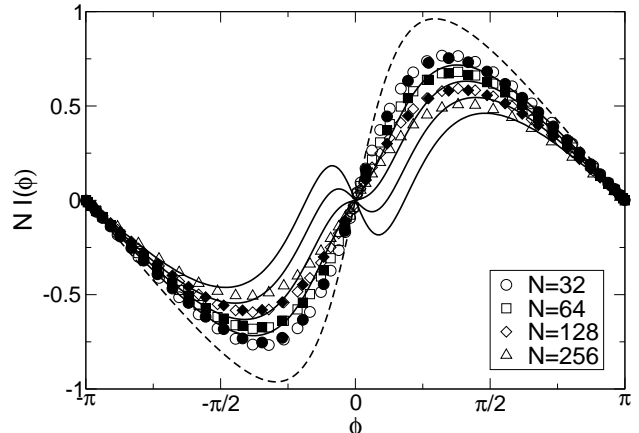


FIG. 3. Persistent current $NI(\phi)$ for $U = 1$, $\rho = 0.5$, and different N . The filled symbols are DMRG data, the open symbols RG data, and the solid lines are obtained from a Hartree-Fock calculation (for the same N). The dashed line is the $U = 0$ result Eq. (7).

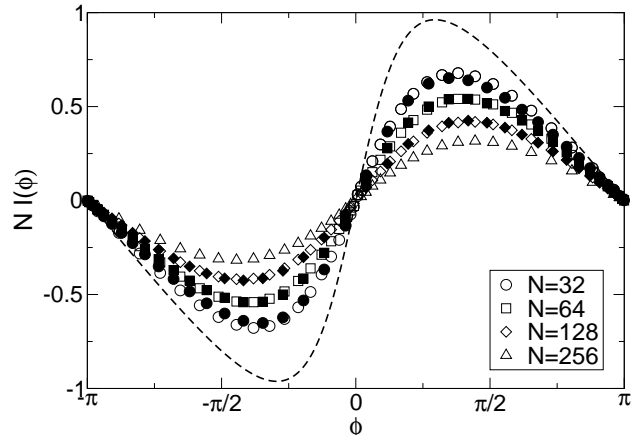


FIG. 4. The same as in Fig. 3, but for $U = 1.73333$, $\rho = 0.5$ and without Hartree-Fock results.

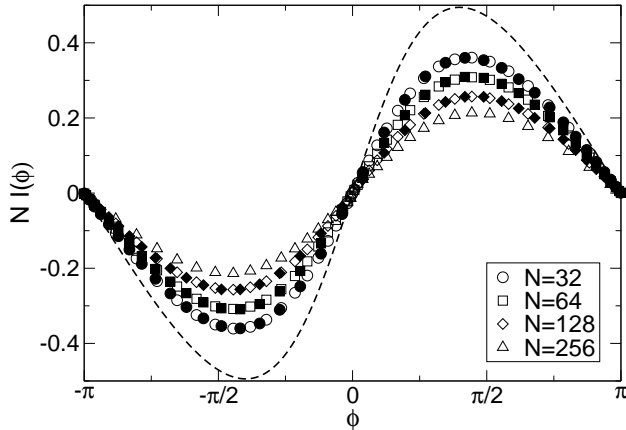


FIG. 5. The same as in Fig. 3, but for $U = 1$, $\rho = 0.25$ and without Hartree-Fock results.

To analyze our data in more detail we have numerically determined the coefficients I_k (for $k = 1, 2, 3$) of a Fourier expansion

$$I(\phi) = \sum_{k=1}^{\infty} I_k \sin(k\phi) \quad (20)$$

for different U , ρ , and N . From bosonization one expects, that NI_k for $k = 1$ decays asymptotically as $N^{-\alpha_B}$ and that the higher order Fourier coefficients die off even faster. To better understand the behavior of NI_k for $k = 2$ and 3 we will use the one-particle picture mentioned in the introduction. According to this many bosonization results can be understood in terms of an effective $|T(k_F)|$ which is suppressed by a factor $N^{-\alpha_B}$ compared to the non-interacting transmission amplitude. Using this and Eq. (8) one concludes that NI_k (at least for $k = 2$ and 3) should decay as $N^{-k\alpha_B}$. This argument is based on the use of a single particle picture and needs further justification. Fig. 6 shows $\ln[NI_k]$ ($k = 1, 2, 3$) as a function of $\ln[N]$ for $U = 1$, $\rho = 0.25$ and Fig. 7 contains data for $U = 1.73333$, $\rho = 0.5$. In addition to the DMRG and RG data straight lines with slope $-k\alpha_B$ [see Eq. (3)] (solid lines) and $-k\alpha_B^{\text{RG}}$ (dashed lines) for $k = 1, 2, 3$ are shown. Since the flow of the two-particle vertex has been neglected in the functional RG, within this approach we can only expect exponents to be correct to leading order in U . α_B^{RG} is the boundary exponent of the local spectral weight (close to the boundary) as we have determined it in Refs. 33 and 34 using the RG for much larger system sizes. As expected it agrees with α_B only to leading order in U . For $U = 1$ we have $\alpha_B^{\text{RG}} = 0.291$ instead of $\alpha_B = 1/3$ and for $U = 1.73333$, $\alpha_B^{\text{RG}} = 0.475$ instead of $\alpha_B = 0.667$. From both figures it is clear that higher order Fourier coefficient decay faster than lower ones. On the other hand only the data obtained for a already fairly strong bare impurity $\rho = 0.25$ follow at large N lines with the expected exponents (see Fig. 6). Even in this case the DMRG data for larger N have to bend further down to reach the predicted behavior (slope $\sim -k\alpha_B$). For large N also the

behavior of the $k = 2$ and 3 Fourier coefficients seems to be consistent with the above predictions obtained using the one-particle language. For $\rho = 0.5$ - an impurity of intermediate strength - even for large $U = 1.73333$ and up to $N = 128$ respectively $N = 256$ lattice sites the DMRG and RG data still show a strong curvature. For this case the bosonization prediction cannot be demonstrated unambiguously although the data show a tendency towards a behavior which is consistent with this prediction. Results for $U = 1$, $k = 1$, and different ρ are summarized in Fig. 8. The bare transmission for $\rho = 0.9$ is $|T(k_F)|^2 = 0.99$ at $U = 0$ and for $\rho = 0.1$ we have $|T(k_F)|^2 = 0.04$. These findings are consistent with the results obtained for a local observable - the spectral weight close to the impurity.^{33,34}

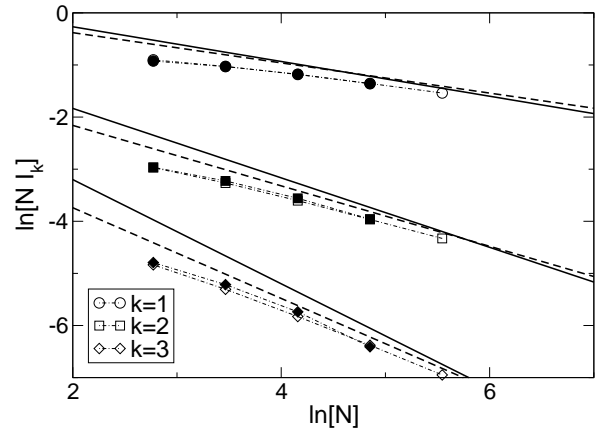


FIG. 6. $\ln[NI_k]$ as a function of $\ln[N]$ for $U = 1$, $\rho = 0.25$, and $k = 1, 2, 3$. The filled symbols are DMRG data and the open symbols RG data. The solid lines have slope $-k\alpha_B$ and the dashed ones slope $-k\alpha_B^{\text{RG}}$. The dashed-dotted lines are guides to the eyes. Open symbols which are not seen are hidden by the filled ones.

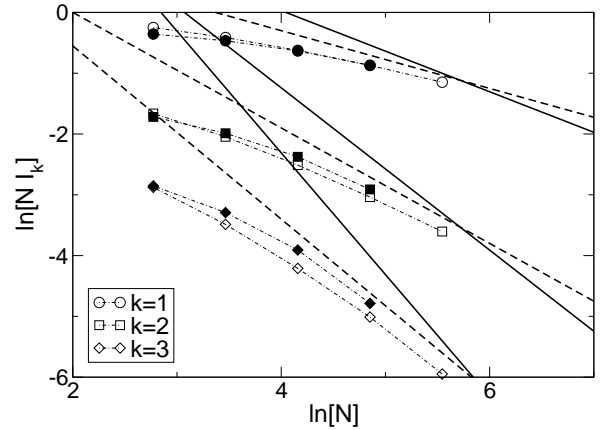


FIG. 7. The same as in Fig. 6, but for $U = 1.73333$, $\rho = 0.5$.

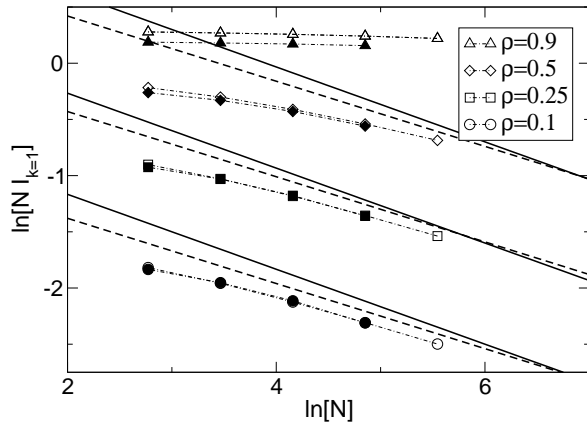


FIG. 8. The same as in Fig. 6, but for $U = 1$, $k = 1$, and different ρ .

One can stress the single particle picture even further and use the non-interacting expression for $I(\phi)$ [Eq. (7)] with an effective transmission amplitude $|T_{\text{eff}}(k_F)|$ as a parameter to fit our data for different U , ρ , and N . For small N this fitting procedure cannot be expected to work as good as for larger ones since Eq. (7) only provides the large N behavior of the current in the non-interacting case. One then expects that $|T_{\text{eff}}(k_F)|$ for $N \rightarrow \infty$ scales as $N^{-\alpha_B}$ (respectively $N^{-\alpha_B^{\text{RG}}}$ for the RG data). Similar to Fig. 8 the effective transmission amplitudes show this behavior only for small ρ and large N . For intermediate to weak impurities the scaling limit is not reached. We have demonstrated that the use of the single particle language can be useful in the present context. Nevertheless it involves arguments which are “hand waving” and we thus do not follow this route any further.

VI. SUMMARY AND PERSPECTIVES

With our work we achieved two goals. We first determined the detailed functional form of the persistent current $I(\phi)$ realized in a lattice model of one-dimensional interacting electrons penetrated by a magnetic flux in the presence of a single impurity. This enabled us to go beyond the large N scaling limit in which the current is proportional to $\sin \phi$ and vanishes as $N^{-\alpha_B-1}$, and investigate the corrections to this behavior. Only for large bare impurities and large system sizes we were able to confirm the bosonization prediction. For intermediate to weak impurities the asymptotic limit described by bosonization is not reached for systems of up to 256 lattice sites and the current shows a more complex behavior. These results are consistent with our observations for the local spectral weight close to an impurity.^{33,34} By comparing the high precision DMRG data to the ones obtained within a functional RG approach, where the flow of the two-particle vertex was neglected, we moreover demonstrated that the latter method can to a very high accuracy also be used for global observables such

as the persistent current. This holds for interactions as large as the band width. Our results show that even in the cases where the universal scaling limit is not reached correlation effects included in the RG are still very important. This is demonstrated by a comparison to results obtained with the Hartree-Fock approximation which are qualitatively wrong.

Besides the hopping impurities we have also studied the case of a single site impurity³³ for selected parameter sets and obtained results which are comparable to the ones presented above.

The functional RG can be applied to other microscopic models (including e.g. long range interaction), at finite temperatures, and for models with disorder. We expect that including the flow of the two-particle vertex - as discussed for the local spectral weight in Ref. 46 - will further increase the accuracy of the RG data for the persistent current. The flow of the interaction vertex is of special importance for models with spin since in Luttinger liquids with spin the flow of the electron-electron backscattering has to be taken into account.⁴⁷ It should thus be included in further applications of the RG method on one-dimensional models. Considering currents driven by a small difference in voltage within the RG it is also possible to include leads and to realize a great variety of electronic circuits. It can be expected that in small conducting molecular systems of the size of a few ten to a few hundred lattice sites which in the near future will be accessible to experiments correlation effects will be important but the asymptotic limit described by the effective field theory will not be reached. The RG is an ideal tool to investigate the electronic properties of such systems.

ACKNOWLEDGEMENTS

We would like to thank M. Henkel, H. Schoeller, W. Metzner, and K. Schönhammer for very valuable discussions and P. Schmitteckert for comments on the manuscript. U.S. is grateful to the Deutsche Forschungsgemeinschaft for support from the Gerhard-Hess-Preis and V.M. acknowledges support from the Bundesministerium für Bildung und Forschung (Juniorprofessor Programm).

¹ L.P. Lévy, G. Dolan, J. Dunsmuir, and H. Bouchiat, Phys. Rev. Lett. **64**, 2074 (1990).

² V. Chandrasekhar, R.A. Webb, M.J. Brady, M.B. Ketchen, W.J. Gallagher, and A. Kleinsasser, Phys. Rev. Lett. **67**, 3578 (1991).

³ D. Mailly, C. Chapellier, and A. Benoit, Phys. Rev. Lett. **70**, 2020 (1993).

- ⁴ B. Reulet, M. Ramin, H. Bouchiat, and D. Mailly, Phys. Rev. Lett. **75**, 124 (1995).
- ⁵ E.M.Q. Jariwala, P. Mohanty, M.B. Ketchen, and R.A. Webb, Phys. Rev. Lett. **86**, 1594 (2001).
- ⁶ W. Rabaud, L. Saminadayar, D. Mailly, K. Hasselbach, A. Benoît, and B. Etienne, Phys. Rev. Lett. **86**, 3124 (2001).
- ⁷ see e.g. U. Eckern and P. Schwab, J. of Low Temp. Physics **126**, 1291 (2002) and references therein.
- ⁸ M. Abraham and R. Berkovits, Phys. Rev. Lett. **70**, 1509 (1993).
- ⁹ G. Bouzerar, D. Poiblanç, and G. Montambaux, Phys. Rev. B **49**, 8258 (1994).
- ¹⁰ H. Kato and D. Yoshioka, Phys. Rev. B **50**, 4943 (1994).
- ¹¹ A. Cohen, K. Richter, and R. Berkovits, Phys. Rev. B **57**, 6223 (1998).
- ¹² A.O. Gogolin and N.V. Prokof'ev, Phys. Rev. B **50**, 4921 (1994).
- ¹³ M. Henkel and D. Karevski, Eur. Phys. J. B **5**, 787 (1998).
- ¹⁴ S. Jaimungal, M.H.S. Amin, and G. Rose, Int. J. of Mod. Phys. B **13**, 3171 (1999).
- ¹⁵ F.D.M. Haldane, J. Phys. C **14**, 2585 (1981).
- ¹⁶ M. Schick, Phys. Rev. **166**, 404 (1968). The author only considers the case of the one-dimensional electron gas with quadratic dispersion. This model is Galilean-invariant which implies that $v_J = v_F$ independent of the interaction, where v_F is the Fermi velocity.
- ¹⁷ D. Loss, Phys. Rev. Lett. **69**, 343 (1992).
- ¹⁸ A. Luther and I. Peschel, Phys. Rev. B **9**, 2911 (1974).
- ¹⁹ D.C. Mattis, J. Math. Phys. **15**, 609 (1974).
- ²⁰ W. Apel and T.M. Rice, Phys. Rev. B **26**, 7063 (1982); T. Giamarchi and H.J. Schulz, *ibid.* **37**, 325 (1988).
- ²¹ C.L. Kane and M.P.A. Fisher, Phys. Rev. B **46**, 15233 (1992).
- ²² S. Eggert and I. Affleck, Phys. Rev. B **46**, 10866 (1992).
- ²³ D. Yue, L. I. Glazman, and K. A. Matveev, *Phys. Rev. B* **49**, 1966 (1994).
- ²⁴ V. Meden, W. Metzner, U. Schollwöck, O. Schneider, T. Stauber, and K. Schönhammer, Eur. Phys. J. B **16**, 631 (2000).
- ²⁵ P. Schmitteckert, Ph.D. Thesis, Augsburg, 1996.
- ²⁶ P. Schmitteckert, T. Schulze, C. Schuster, P. Schwab, and U. Eckern, Phys. Rev. Lett. **80**, 560 (1998).
- ²⁷ T.M.R. Byrnes, R.J. Bursill, H.-P. Eckerle, C.J. Hamer, and A.W. Sandvik, cond-mat/0205140 (2002).
- ²⁸ $\phi = \pi$ corresponds to so called anti-periodic boundary conditions and the hamiltonian matrix remains real.
- ²⁹ Similar studies have been performed by F. Carvalho Dias, M. Henkel, and I.R. Pimentel (to be published).
- ³⁰ C. Wetterich, Phys. Lett. B **301**, 90 (1993).
- ³¹ T. R. Morris, Int. J. Mod. Phys. A **9**, 2411 (1994).
- ³² D. Zanchi and H. J. Schulz, Phys. Rev. B **61**, 13609 (2000); C. J. Halboth and W. Metzner, *ibid.* **61**, 7364 (2000); C. Honerkamp, M. Salmhofer, N. Furukawa, and T. M. Rice, *ibid.* **63**, 5109 (2001).
- ³³ V. Meden, W. Metzner, U. Schollwöck, and K. Schönhammer, Phys. Rev. B **65**, 045318 (2002).
- ³⁴ V. Meden, W. Metzner, U. Schollwöck, and K. Schönhammer, J. of Low Temp. Physics **126**, 1147 (2002).
- ³⁵ T. Busche, L. Bartosch, and P. Kopietz, cond-mat/0202175 (2002).
- ³⁶ H.-F. Cheung, Y. Gefen, E.K. Riedel, and W.-H. Shih, Phys. Rev. B **37**, 6050 (1988).
- ³⁷ F.D.M. Haldane, Phys. Rev. Lett. **45**, 1358 (1980).
- ³⁸ S. Qin, M. Fabrizio, L. Yu, M. Oshikawa, and I. Affleck, Phys. Rev. B **56**, 9766 (1997).
- ³⁹ V. Meden, P. Schmitteckert, and N. Shannon, Phys. Rev. B **57**, 8878 (1998).
- ⁴⁰ A.A. Abrikosov, L.P. Gorkov, and I.E. Dzyaloshinski, *Methods of quantum field theory in statistical physics* (Dover Publishing, New York, 1975).
- ⁴¹ S.R. White, Phys. Rev. Lett. **69**, 2863 (1992); *Density-Matrix Renormalization*, ed. by I. Peschel, X. Wang, M. Kaulke, and K. Hallberg (Springer, Berlin, 1999).
- ⁴² There is a misprint in Eq. (3) of Ref. 34. The first minus sign on the right hand side has to be replaced by a plus.
- ⁴³ A. Schmid, Phys. Rev. Lett. **66**, 80 (1991).
- ⁴⁴ B.L. Altshuler, Y. Gefen, and Y. Imry, Phys. Rev. Lett. **66**, 88 (1991).
- ⁴⁵ W.H. Press, B.P. Flannery, S.T. Teukolsky, and W.T. Vetterling, *Numerical Recipes* (Cambridge University Press, Cambridge, 1986).
- ⁴⁶ S. Andergassen, V. Meden, W. Metzner, U. Schollwöck, and K. Schönhammer, to be published.
- ⁴⁷ J. Sólyom, Adv. Phys. **28**, 201 (1979).